===================== **PHOTOCHEMISTRY** =====================

Spectral and Photochemical Properties of Hybrid Organic−Inorganic Nanosystems Based on CdS Quantum Dots and a Styrylquinoline Ligand

M. F. Budyka and O. V. Chashchikhin

Institute of Problems of Chemical Physics, Russian Academy of Sciences,
pr. Akademika Semenova 1, Chernogolovka, Moscow oblast, 142432 Russia
e-mail: budyka@icp.ac.ru
Received November 13, 2015

Abstract—The kinetics of photolysis of a styrylquinoline (SQ) derivative as the photochromic ligand in organic−inorganic hybrid nanosystems (HNSs) with the core composed of CdS quantum dots (QDs) has been studied for the first time as a function of the number of ligand molecules in the HNS shell, which varied from 1 to 10. The hybrid nanosystems have been synthesized in the microwave-assisted mode according to the single-step injection-free procedure. It has been shown that high quantum yields of photoisomerization of the SQ ligand are conserved in the HNS. In the early stages of the photolysis, regardless of the number of SQ ligand molecules in the HNS shell, the kinetics obeys the equation for the photolysis of the monomolecular system (model SQ photochrome) with allowance for the absorption due to QDs as an inert shutter. During the course of long-term photolysis, the quantum dots undergo photodegradation to be completely decomposed. According to the principal component analysis data, several photoproducts with different absorption spectra are formed at the intermediate times of the HNS photolysis.

Hybrid organic−inorganic nanosystems (**HNS**s, conjugates) attract attention of scientists due to the possibility of combination of the useful properties of both constituents, the inorganic component, a quantum dot (**QD**), and the organic component, a ligand (**LH**). By acting on the ligand, the processes of electron or energy transfer between the organic and inorganic components and, hence, the properties of the HNS as a whole can be controlled [1−4]. Hybrid organic−inorganic nanosystems in which the organic ligand contains photochromic groups are especially attractive, because QD fluorescence in these systems can be controlled by illuminating with light, which converts the photochrome from one isomeric state to another [5−8].

As a rule, the properties of light-controlled systems are studied at the binary 0−1 or on−off level. The problems of the photolysis kinetics of the photoactive ligand in the HNS composition or the possible dependence of the photoisomerization quantum yield of the photochrome and the composition of the photostationary state on the presence of other photochromes are not considered. At the same time, it is known that the efficiency of Förster resonance energy transfer (**FRET**) in these systems depends on the number of ligand molecules in the HNS organic shell, and it is the photochrome isomerization that is used to control the FRET process [9].

In this work, the aspects concerning the dependence of the photochemical properties of HNSs on the number of organic ligand molecules in the HNS composition was studied using the example of systems of the general formula QDL_n, where QD is the CdS quantum dot of a 2.4 nm diameter, L is the deprotonated residue (thiolate ion) of the ligand with the styrylquinoline (SQ) moiety, and n is the number of ligand molecules in the HNS shell. As the photoactive LH ligand, (*E*)-2-(4-[9-mercaptononoxy]styryl)quinoline was used, in which the photochromic SQ is linked by a polymethylene chain with the mercaptan (thiol) group playing the role of the anchor for fixing on the QD surface. Benzylmercaptan (**BzM**) was used as an inert QD-stabilizing (supporting) ligand . The schematic structure of the nanosystem and the structures of the inert and photoactive ligands are shown in Scheme 1.
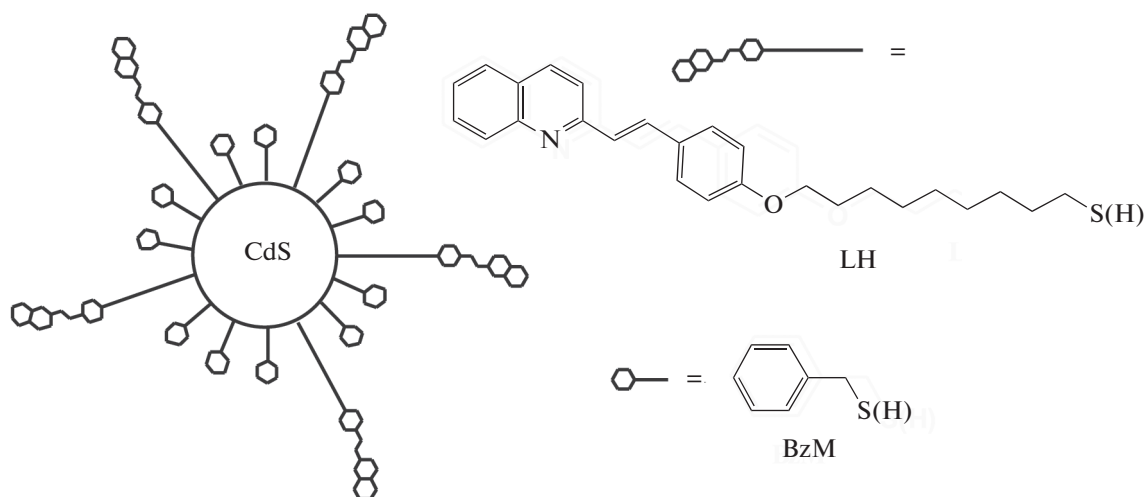
Scheme 1. Schematic structure of the QDL$_n$ hybrid nanosystem and the structures of the ligands, benzylmercaptan (BzM) and (*E*)-2-(4-[9-mercaptononoxy]styryl)quinoline (LH). The ratio between the sizes of separate components corresponds to real sizes (see text).

EXPERIMENTAL

The hybrid organic–inorganic nanosystems were synthesized in the microwave-assisted mode using the single-step injection-free procedure described in [11], which was slightly modified. First, thiourea was reacted with a ligand whose polymethylene chain was end-capped with the bromine atom, which was replaced by the mercapto group under microwave activation to afford in situ the desired ligand in the form of thiouronium salt. Then, the inert ligand BzM and cadmium acetate were added to the reaction mixture, and the mixture was subjected to microwave irradiation again. The concentrations of ligands and precursors were chosen to form QDL$_n$ hybrid systems, in which the QD had the size of 2.4 nm, and $n = 1.1$ (HNS1) and $n = 9.5$ (HNS2). The composition was determined from absorption spectra (see below).

The absorption spectra were recorded on a Specord M-400 spectrophotometer. All experiments were carried out at room temperature in air-saturated DMF solutions in quartz cells with an optical path length of $l = 1$ cm. Light-emitting diodes SETI UVTOP-355-TO-18-HS (LED-370, $\lambda_{max} = 370$ nm, FWHM = 14 nm) and SETI UVTOP-310-TO-39-HS (LED-316, $\lambda_{max} = 316$ nm, FWHM = 11 nm) were used as a source of UV light. The light intensity measured with a ferrioxalate actinometer was $(1.07-1.13) \times 10^{-9}$ and $(4.5-5.5) \times 10^{-10}$ einstein cm^{-2} s^{-1} for LED-370 and

LED-316, respectively. The error in measurement of photoisomerization quantum yields was 20%.

RESULTS AND DISCUSSION

Spectral Properties

Figure 1 shows the normalized absorption spectra of the test nanosystems and the model compounds. Spectrum *1* characterizes the CdS quantum dots with the shell composed of the supporting BzM alone (without the photoactive ligand). A maximum of the long-wavelength absorption band (337 nm) corresponds to the QD diameter of 2.4 nm. The molar absorption coefficient at the maximum is 8×10^4 L mol^{-1} cm^{-1} [11]. Spectrum *2* is the spectrum of the free ligand, LH = , (*E*)-2-(4-[9-mercaptononoxy]styryl)quinoline, with a maximum of the long-wavelength absorption band at 359 nm and the molar absorption coefficient at the maximum of 2.65×10^4 L mol^{-1} cm^{-1}. Spectra *3* and *4* belong to HNS1 and HNS2, respectively. It is clear that the long-wavelength absorption band at 360 nm is due to the SQ photochrome because the molar absorption coefficient of QD at 359 nm is below that of LH by a factor of 13.

The approximation of the experimental spectra for the nanosystems by the spectra of free QD and LH makes it possible to determine the HNS composition. On the assumption that the QD and LH spectra are not changed by binding the components in the united hybrid nanosystem, absorbance A_{QDL} for QDL$_n$ nanosystems is defined as follows:

$$A_{QDL} = \varepsilon_{QDL} c_{QDL} l = (\varepsilon_{QD} + n\varepsilon_L) c_{QDL} l,$$

where ε_i is the molar absorption coefficient of the *i*th component, c_{QDL} is the HNS concentration, and l is
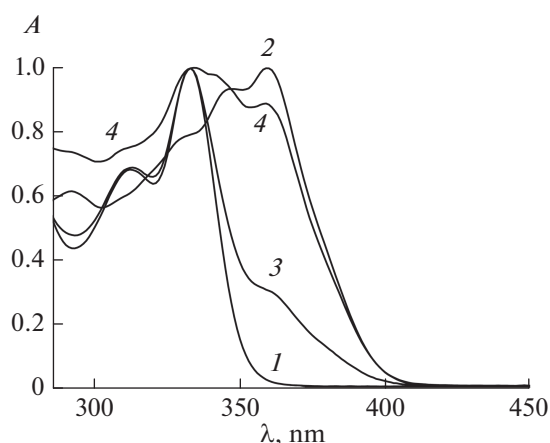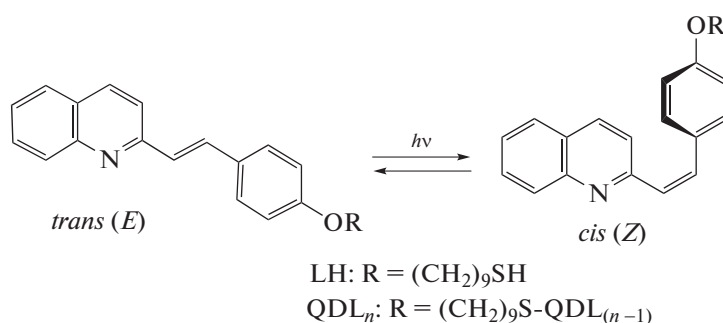
Fig. 1. Absorption spectra in DMF: (*1*) CdS quantum dot of a 2.4 nm diameter , (*2*) LH ligand (*E*)-2-(4-[9-mercaptononoxy]styryl)quinoline, (*3*) HNS1, and (*4*) HNS2; the spectra are normalized relative to a maximum.

the optical path length. This equation involves two unknown parameters n and c. The parameter c can be excluded by normalizing the absorption spectrum (absorbance A_λ at a wavelength λ) relative to the maximum at 333 nm.

$$A_{calc,\lambda,norm} = (\varepsilon_{QD} + n\varepsilon_{LH})_\lambda / (\varepsilon_{QD} + n\varepsilon_{LH})_{max},$$

$$A_{exp,\lambda,norm} = A_{exp,\lambda} / A_{exp,max}.$$

The value of n was found by minimizing the root-mean-square deviation (ΔA) of the calculated spectrum from the experimental one over the entire wavelength range

$$\Delta A = \left(\Sigma \left(A_{calc,\lambda,norm} - A_{exp,\lambda,norm} \right)^2 / m \right)^{1/2},$$

where m is the number of data points (wavelengths) in the experimental absorption spectra of QDL_n. The calculated average number of the SQ ligands in the QD shell (n) is 1.1 or 9.5 in HNS1 or HNS2, respectively.

It should be pointed out that this is the average value of n. These systems can be characterized by a Poisson distribution [12], according to which 33% "empty" QDs (free of the SQ ligand), 37% HNS with one ligand, 20% HNS with two ligands, and so on are present in the HNS1 solution with $n = 1.1$. When $n = 9.5$ (HNS2), the highest proportion of the nanosystems containing 9 SQ ligand molecules is 13% and the nanosystems containing 8 and 10 SQ ligand molecules make 12% each.

Photochemical Properties

Both the LH ligand and QDL_n hybrid systems contain the photoactive SQ moiety, which can undergo the reversible photoisomerization reaction between the *trans* (*E*)- and *cis* (*Z*)-isomers (Scheme 2).

LH: R = (CH$_2$)$_9$SH
QDL_n: R = (CH$_2$)$_9$S-QDL$_{(n-1)}$

Scheme 2. Photoisomerization of the SQ moiety of the free ligand LH and the hybrid QDL_n nanosystem, where QD is a CdS nanocrystal (quantum dot).

The photolysis of free LH in DMF occurred similarly to that of the SQ photochrome in other solvents [13, 14]. Irradiation resulted in spectral changes characteristic of photoisomerization, which were stopped after reaching the photostationary state (PS). The PS composition and the spectrum of the free *cis*-isomer were calculated by the Fischer method [15].

The HNS photolysis was studied using light at a wavelength of 370 nm in the SQ photochrome absorption range and 316-nm light in the range of absorption by the system as a whole with predominance of QDs. Figure 2 shows the spectral changes observed during the photolysis of HNS1, with the absorbance kinetics

being depicted in insets. In the case of 370-nm photolysis (Fig. 2a), two distinct time intervals are observed: first, the fast reaction evidently associated with the photoisomerization of the SQ photochrome occurs, and the rate curve reaches a quasi-PS plateau. During the course of further photolysis, the absorbance slowly decreases because of quantum dot degradation, since the characteristic QD absorption band at 330 nm disappears completely. In the case of 315-nm photolysis (Fig. 2b), the QD degradation rate is comparable with the ligand photolysis rate, as the spectral changes occur uniformly throughout the entire wavelength range and there are no clearly observed breaks in the
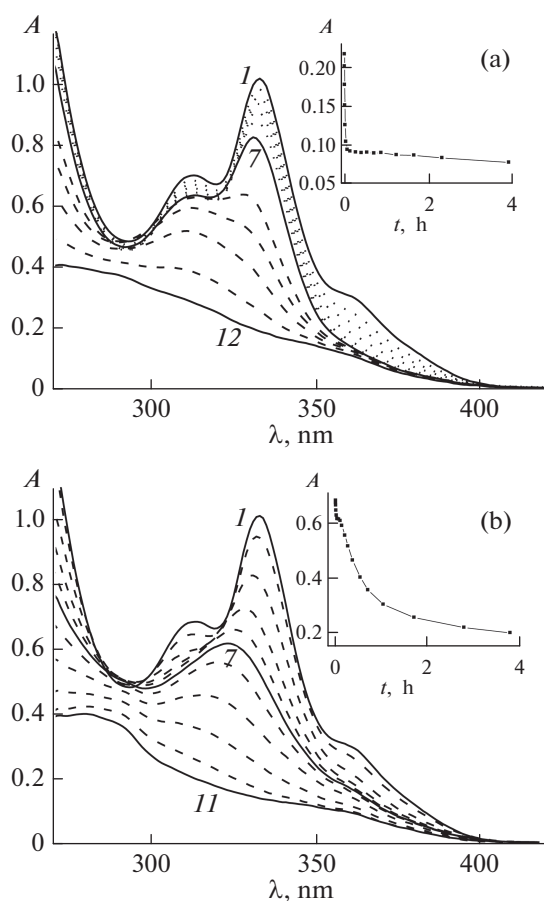
Fig. 2. Evolution of absorption spectra in the photolysis of HNS1 in DMF at (a) 370 nm; intensity 1.1×10^{-9} einstein $\mathrm{cm}^{-2}\mathrm{s}^{-1}$; photolysis time, s: 0 (*1*), 15 (*2*), 30 (*3*), 60 (*4*), 120 (*5*), 240 (*6*), 480 (*7*), 1440 (*8*), 2520 (*9*), 4440 (*10*), 8340 (*11*), and 14040 (*12*) and (b) 316 nm; intensity 4.5×10^{-10} einstein $\mathrm{cm}^{-2}\mathrm{s}^{-1}$; photolysis time, s: 0 (*1*), 30 (*2*), 120 (*3*), 240 (*4*), 360 (*5*), 480 (*6*), 720 (*7*), 1320 (*8*), 2520 (*9*), 6120 (*10*), and 13620 (*11*). Insets: photolysis kinetics at the irradiation wavelengths.

Fig. 3. Evolution of absorption spectra in the photolysis of HNS2 in DMFA at (a) 370 nm; intensity 1.1×10^{-9} einstein $\mathrm{cm}^{-2}\mathrm{s}^{-1}$; photolysis time, s: 0 (*1*), 5 (*2*), 15 (*3*), 30 (*4*), 60 (*5*), 120 (*6*), 480 (*7*), 1440 (*8*), 2640 (*9*), 5160 (*10*), and 19200 (*11*) and (b) 316 nm; intensity 4.5×10^{-10} einstein $\mathrm{cm}^{-2}\mathrm{s}^{-1}$; photolysis time, s: 0 (*1*), 15 (*2*), 60 (*3*), 120 (*4*), 300 (*5*), 420 (*6*), 600 (*7*), 1020 (*8*), 1920 (*9*), 3720 (*10*), 5520 (*11*) and 12720 (*12*). Insets: photolysis kinetics at the irradiation wavelengths.

rate curve. Model investigations have shown that the photodegradation of QDs is not due to the presence of the SQ ligand in the HNS shell. At the same durations of photolysis of the "clean" QD with the shell composed of BzM molecules alone, spectral changes were similar to those shown in Fig. 2: a decrease in the intensity of the QD absorption band with its simultaneous broadening and hypsochromic shift.

The spectral changes observed in the photolysis of HNS2 are shown in Fig. 3, the absorbance kinetics is depicted in insets. As in the case of HNS1 photolyzed at 370 nm (Fig. 3a), two portions can be distinguished in the rate curve: the first due to the fast photoisomerization of the SQ photochrome to reach a quasi-photostationary state followed by the slow degradation of the quantum dot (Fig. 3a, inset). In the 316-nm photolysis of HNS2 (Fig. 3b), the spectral changes also can be divided in two ranges and the rate curve has the
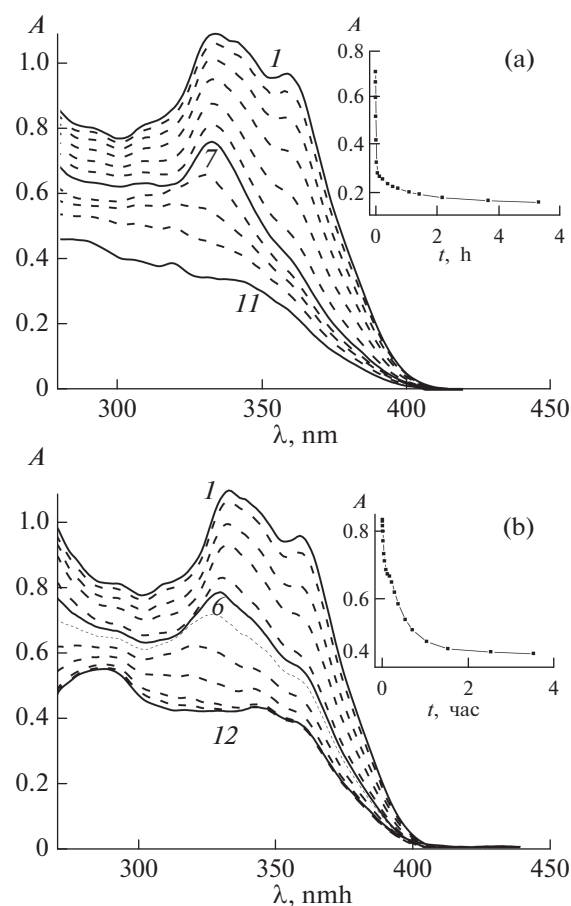
typical form with a break (Fig. 3b, inset). This differs HNS2 from HNS1.

The occurrence of different reactions during the irradiation of the nanosystems is clearly revealed by processing the spectral data using the principal component analysis (PCA) [16]. Figure 4 shows score plots in which the experimental points are presented in the basis of the first two singular vectors. Every point in the plot corresponds to a particular spectrum of the reaction mixture in the photolysis. The spectral range of 270–450 nm with a step size of 2 nm was taken into account; i.e., the initial matrix included 181 absorbance values for each spectrum.

The principal component analysis shows that , several reactions involving several chromophores occur in all the systems. Three of the chromophores are evident; these are the QD and the SQ photochrome *trans*- and *cis*-isomers. During the photoisomeriza-

tion reaction when the concentrations of only two chromophores, the *trans*- and *cis*-isomers, vary in the system, the experimental data points in PCA fall in a straight line between the spectra of these isomers. In the separate analysis of the initial portion of the spectral changes for HNS1 in the basis of seven initial spectra (Fig. 4a, inset), the experimental spectra in the case of 370-nm photolysis (*1*) first fall in the straight line, characterizing the (fast) photoisomerization of the ligand. Then, the data points deviate, since the fourth chromophore that characterizes the product of the (slow) QD photodegradation appears in the solution. In the case of 316-nm photolysis, the ligand photoisomerization and QD photodegradation occur at comparable rates, resulting in spectral changes of another type in the initial portion (curve *2*, inset), and the PCA plot is directed to the opposite side. The complex shape of the curves in Fig. 4 indicates that several reactions associated with the photodegradation of the QD and, possibly, the SQ ligand occur during the long-term photolysis.

The principal component analysis of the data for HNS2 (Fig. 4b) shows that the spectral changes in both cases are alike, but the photoisomerization initially proceeds more selectively during the photolysis at 370 nm (straight line segment of curve *1*) and the QD degradation is observed already in the early stages during irradiation with 316-nm light (curve *2*).

Photolysis Kinetics

The kinetics of reversible photoisomerization of the LH ligand obeys differential equation (1):

$$dA/dt = -(\varepsilon_t - \varepsilon_c)(\varphi_{tc}A_t - \varphi_{ct}A_c) \times \left(1 - 10^{-A}\right)I_0/A, \tag{1}$$

where $A = A_t + A_c$, A_i and ε_i are the absorbance and the molar absorption coefficient of the ith (*trans* or *cis*) isomer at the irradiation wavelength, respectively; φ_{tc} and φ_{ct} are the quantum yields of *trans-cis* and *cis-trans* photoisomerization; and I_0 is the intensity of the acting light. The quantum yields given in the table for LH were calculated by numerical integration of Eq. (1) with minimization of the deviation between calculated and experimental absorbance values (for the calculation procedure, see [17]). A comparison with the data for other solvents shows that the quantum yields of SQ chromophore photoisomerization in DMF are close to those in ethanol ($\varphi_{tc} = 0.56$, $\varphi_{ct} = 0.43$) [13] and are higher than those for the reaction in chloroform ($\varphi_{tc} = 0.21$, $\varphi_{ct} = 0.14$) [14].

Let us consider the photolysis kinetics for QDL_n HNS with n SQ ligands. In the initial state, all the ligands are in the form of the *trans* (*E*)-isomer. This state is designated as $QD(E)_n$. Under irradiation, the successive photoisomerization of the SQ ligands to give the *cis* (*Z*)-isomers:
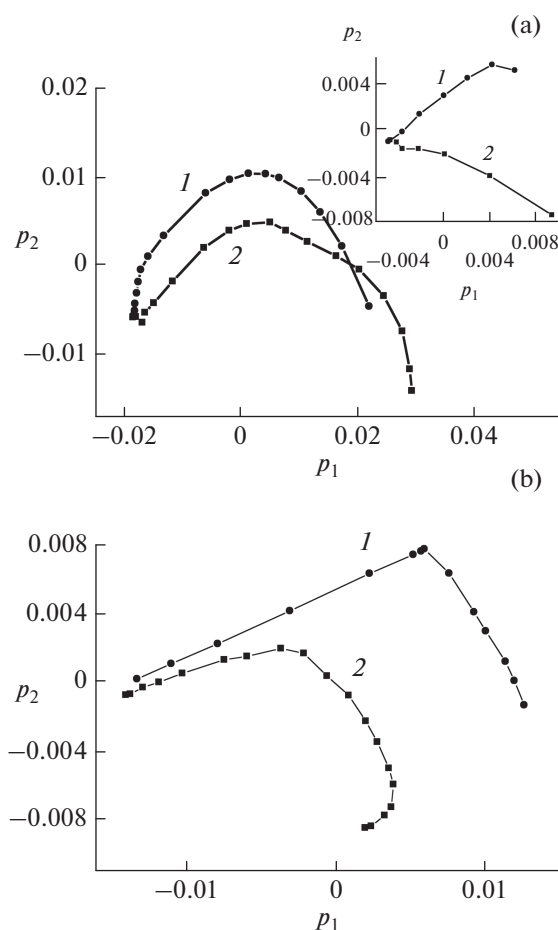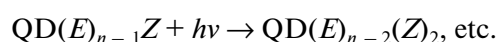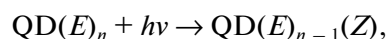

Рис. 4. Principal component analysis of spectral changes during the photolysis of (a) HNS1 and (b) HNS2 at (*1*) 370 and (*2*) 316 nm; the experimental spectra are depicted in the basis of two first singular vectors p_1 and p_2. Inset: principal component analysis of the spectral changes only in the initial period of the HNS1 photolysis (see text).

$$QD(E)_n + h\nu \rightarrow QD(E)_{n-1}(Z),$$

$$QD(E)_{n-1}Z + h\nu \rightarrow QD(E)_{n-2}(Z)_2, \text{ etc.}$$

and corresponding reverse reactions will occur. In the general form, the photoisomerization reaction can be written as

$$QD(E)_{n-m}(Z)_m + h\nu \rightarrow QD(E)_{n-m-1}(Z)_{m+1} + QD(E)_{n-m+1}(Z)_{m-1}.$$
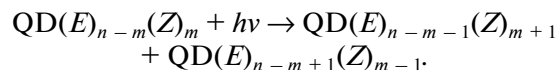
For $QD(E)_n$ HNS, it is necessary to write n reactions; i.e., we get a set of $2n$ differential equations containing $2n$ quantum yields, which need to be determined. This set can be significantly simplified by taking into account that the conversion rate for a given photochrome is proportional to the fraction of light absorbed by this photochrome in the absence of energy transfer between the photochromes in the HNS shell. This fraction is equal to the ratio of the molar absorption coefficient of the photochrome to the molar absorption coefficient of the HNS as a whole.

The quantum yields of the *trans−cis* (φ_{tc}) and *cis−trans* (φ_{ct}) photoisomerization of the free SQ ligand and in the composition of HNS in the photolysis at a wavelength of 370 nm (DMF, ±20%).

Sample	φ_{tc}	φ_{ct}
LH	0.46	0.46
HNS1	0.45	0.78
HNS2	0.47	0.74

Furthermore, as the first approximation, assume that the quantum yields for the same type of reaction—φ_{tc} for the *trans−cis* photoisomerization reaction $(E) \rightarrow (Z)$ and φ_{ct} for the *cis−trans* photoisomerization reaction $(Z) \rightarrow (E)$—are the same for all the nanosystems $QD(E)_{n-m}(Z)_m$ regardless of the values of n and m. In this case, the photolysis kinetics (consumption rate) of the $QD(E)_{n-m}(Z)_m$ isomer can be written as

$$d\left[QD(E)_{n-m}(Z)_m\right]/dt = -((n-m)\varepsilon_t\varphi_{tc}$$
$$+ m\varepsilon_c\varphi_{ct})\left[QD(E)_{n-m}(Z)_m\right]\left(1-10^{-A}\right)I_0/A, \quad (2)$$

where the first term in the parentheses sums all the *trans−cis* photoisomerization reactions (decrease in $(n-m)$ and increase in m) and the second term sums all the *cis−trans* photoisomerization reactions (increase in $(n-m)$ and decrease in m) for $QD(E)_{n-m}(Z)_m$ HNS.

Thus, in the general case, the photolysis of a nanosystem containing n photochromes is determined by a set of n equations of type (2) for the concentration of each $QD(E)_{n-m}(Z)_m$ HNS plus the material balance equation. Even on the assumption that the quantum yields for reactions of the same type are identical, their calculation requires optimization of a very large number of parameters (concentrations of all components of the system).

We suggested that the photoisomerization each photochrome in HNS occurs independently in the initial photolysis stages, and the quantum dot can be treated as an inert shutter, whose absorbance (A_{QD}) does not change and is to be added to the absorbance of the *trans-* and *cis-*isomers of the ligand. The absorbance of the solution in this case is defined by Eq. (3)

$$A = A_t + A_c + A_{QD}. \quad (3)$$

Taking into account that $A_{QD} = $ const, the kinetics of QDL_n HNS photolysis is determined in this case by the same differential equation (1) as for the free ligand LH.

The approximation of the experimental data points by rate curves calculated according to Eq. (1) taking into account Eq. (3) shows that the "quantum dot−inert shutter" model adequately describes the photoisomerization kinetics before reaching the quasi-photostationary state. The values found for the quantum yields are listed in the table.

As follows from the data in the table, the *trans−cis* photoisomerization quantum yields (φ_{tc}) of the ligand are not changed within the measurement error by introducing the SQ ligand into the HNS shell. The quantum yields of the reverse, *cis-trans* photoisomerization reaction (φ_{ct}) increases in HNS. Taking into account the flexibility of the polymethylene chain, we may assume that the increase in φ_{ct} is due to steric hindrance, which is created by the organic shell of the hybrid nanosystem to the nonplanar *cis*-isomer of the SQ ligand. Note that φ_{ct} attains values exceeding 0.5, the limiting value for quantum yields in the diabatic mechanism of photoisomerization [18].

It is known that in the case of photolysis of supramolecular systems containing several identical photochromes, the photoisomerization of the first photochrome can yield a photoproduct having a bathochromically shifted absorption spectrum. As a result, the conditions appear for energy transfer from the initial photochrome to the photoproduct, which becomes a quencher in this case. For example, the quantum yields of the reaction of the second photochromic group in some dyads decrease after photoisomerization of the first group [19, 20]. The *trans*-isomer of the SQ ligand has a bathochromically shifted absorption spectrum in comparison with the *cis*-isomer and theoretically may be the quencher for the latter. However, using the example of bisstyrylquinoline dyads containing two SQ units, we have shown [13] that there is no energy transfer from the *cis*- to the *trans*-isomer. In the case of the HNSs examined in this study, the photolysis rate curves are approximated well by the equation for reversible *trans-cis* photoisomerization so that it can be concluded that the reaction rates (photoisomerization quantum yields) for all the photochromes in the composition of these hybrid nanosystems are the same; i.e., the photoisomerization quantum yield for a particular SQ ligand does not depend on the isomeric state of the other ligands.

As shown above, the photodegradation of the quantum dots is observed at long irradiation times in all cases (Figs. 2, 3). Recently, it has been reported that quantum dots are unstable in the long-term photolysis, although low irradiation doses can deactivate surface defects, thereby enhancing quantum dot luminescence (luminescence "photoactivation" effect upon irradiation) [21, 22]. From our data on the photolysis of the pure quantum dot and the hybrid nanosystems by the short-wavelength light, the quantum yield of the QD photodegradation can be estimated at about 0.01; i.e., it is considerably lower that the photoisomerization quantum yield of the SQ ligand. It is for this reason that the contribution of QD photodegradation in the early stages of photolysis can be ignored (the QD considered as an inert shutter) and the absorbance kinetics obeys Eq. (1).

CONCLUSIONS

The study of the photochemical properties of the hybrid organic−inorganic nanosystems with the core composed of CdS quantum dots surrounded by the organic shell containing one to ten molecules of the photochromic ligand, the styrylquinoline derivative, has shown that the high photoisomerization quantum yields of the SQ ligand is conserved in the composition of the nanosystems. In the early photolysis stages, the photolysis kinetics obeys the equation for the photolysis of the monomolecular system with consideration of the quantum dot absorption as an inert shutter independent of the number of SQ ligand molecules in the nanosystem shell. During the long-term irradiation, the quantum dots undergo photodegradation. According to the principal component analysis, several photoproducts with different absorption spectra are formed in this process. The exhaustive photolysis leads to the complete disappearance of quantum dots in the solution.

REFERENCES

1. Medintz, L. and Mattoussi, H., *Phys. Chem. Chem. Phys.,* 2009, vol. 11, p. 17.
2. Credi, A., *New J. Chem.,* 2012, vol. 36, p. 1925.
3. Freeman, R. and Willner, I., *Chem. Soc. Rev.*, 2012, vol. 41, p. 4067.
4. Avellini, T., Lincheneau, C., Vera, F., Silvi, S., and Credi, A., *Coord. Chem. Rev.*, 2014, vol. 263−264, p. 151.
5. Medintz, I.L., Trammell, S.A., Mattoussi, H., and Mauro J.M., *J. Am. Chem. Soc.* 2004, vol. 126, p. 30.
6. Zhu, L., Zhu, M., Hurst, J.K., and Li, A.D.Q., *J. Am. Chem. Soc.*, 2005, vol. 127, p. 8968.
7. Erno, Z., Yildiz, I., Gorodetsky, B., Raymo, F.M., and Branda N.R., *Photochem. Photobiol. Sci.*, 2010, vol. 9, p. 249.
8. Diaz, S.A., Menendez, G.O., Etchehon, M.H., Giordano, L., Jovin, T.M., and Jares-Erijman, E.A., *ACS Nano.*, 2011, vol. 5, p. 2795.
9. Algar, W.R., Kim, H., Medintz, I.L., and Hildebrandt, N., *Coord. Chem. Rev.*, 2014, vol. 263−264, p. 65.
10. Budyka, M.F., Chashchikhin, O.V., Gavrishova, T.N., Spirin, M.G., and Brichkin S.B., *Nanotechnol. Russ.*, 2014, vol. 9, no. 3/4, p. 116.
11. Budyka, M.F., Chashchikhin, O.V., and Nikulin, P.A., *Nanotechnol. Russ.*, 2016, vol. 11, no. 1/2, p. 78.
12. Morris-Cohen, A.J., Frederick, M.T., Cass, L.C., and Weiss, E.A., *J. Am. Chem. Soc.*, 2011, vol. 133, p. 10146.
13. Budyka, M.F., Potashova, N.I., Gavrishova, T.N., and Lee V.M., *High Energy Chem.*, 2012, vol. 46, p. 309.
14. Budyka, M.F., Chashchikhin, O.V., Gavrishova, T.N., Spirin, M.G., and Brichkin S.B., *Nanotechnol. Russ.*, 2014, vol. 9, no. 3/4, p. 116.
15. Gade, R. and Porada, T. *J. Photochem. Photobiol. A: Chem.*, 1997, vol. 107, p. 27.
16. Budyka, M.F., Potashova, N.I., Gavrishova, T.N., and Lee V.M., *High Energy Chem.*, 2010, vol. 44, p. 404.
17. Budyka, M.F., Potashova, N.I., Gavrishova, T.N., and Lee V.M., *High Energy Chem.*, 2008, vol. 42, p. 446.
18. Budyka, M.F., *Russ.Chem. Rev.,* 2012, vol. 81, p. 477.
19. Budyka, M.F., Laukhina, O.D., and Gavrishova T.N. *Mendeleev Commun.*, 1998, vol. 8, no. 2, p. 59.
20. Jacquemin, D., Perpete, E.A., Maurel, F., and Perrier, A., *J. Phys. Chem. C.*, 2010, vol. 11., p. 9489.
21. Carrillo-Carrion, C., Cardenas, S., Simonet, B.M., and Valcarcel, M., *Chem. Commun.*, 2009, vol. 35., p. 5214.
22. Spirin, M.G., Brichkin, S.B., and Razumov, V.F., *High Energy Chem.*, 2015, vol. 49, p. 426.

Translated by T. Nekipelova

SPELL: 1. OK